

# 1 **The Toxin Antitoxin MazEF Drives *Staphylococcus aureus* Chronic Infection**

2  
3 Running Title: MazF drives chronic infection

4  
5 Dongzhu Ma<sup>1</sup>, Jonathan B. Mandell<sup>1</sup>, Niles P. Donegan<sup>2</sup>, Ambrose L. Cheung<sup>2</sup>, Wanyan Ma<sup>1</sup>,  
6 Scott Rothenberger<sup>3</sup>, Robert M. Q. Shanks<sup>4</sup>, Anthony R. Richardson<sup>5</sup>, Kenneth L. Urish<sup>6\*</sup>

7  
8 <sup>1</sup>Arthritis and Arthroplasty Design Group, Department of Orthopaedic Surgery, College of  
9 Medicine, University of Pittsburgh, Pittsburgh, Pennsylvania, United States of America

10  
11 <sup>2</sup>Department of Microbiology and Immunology, Geisel School of Medicine at Dartmouth,  
12 Hanover, New Hampshire, United States of America

13  
14 <sup>3</sup>Clinical and Translation Science Institute; Department of Medicine, University of Pittsburgh,  
15 Pittsburgh, Pennsylvania, United States of America

16  
17 <sup>4</sup>Department of Ophthalmology, University of Pittsburgh, Pittsburgh, Pennsylvania, United  
18 States of America

19  
20 <sup>5</sup>Department of Microbiology and Molecular Genetics, University of Pittsburgh, Pittsburgh,  
21 Pennsylvania, United States of America

22  
23 <sup>6</sup>Arthritis and Arthroplasty Design Group, The Bone and Joint Center, Magee Womens  
24 Hospital of the University of Pittsburgh Medical Center; Department of Orthopaedic Surgery,  
25 Department of Bioengineering, and Clinical and Translational Science Institute, University of  
26 Pittsburgh; Department of Biomedical Engineering, Carnegie Mellon University, Pittsburgh, PA,  
27 15219; urishk2@upmc.edu

28  
29 Corresponding Author: Dr. Kenneth Urish is supported in part by the National Institute of  
30 Arthritis and Musculoskeletal and Skin Diseases (NIAMS K08AR071494), the National Center  
31 for Advancing Translational Science (NCATS KL2TR0001856), the Orthopaedic Research and  
32 Education Foundation, and the Musculoskeletal Tissue Foundation. urishk2@upmc.edu

33  
34 This study was performed at the Departments of Orthopaedic Surgery at the University of  
35 Pittsburgh, Pittsburgh, PA, USA

36  
37  
38 Key Words: Toxin-antitoxin (TA) systems; Biofilm; MazF; *icaADBC*; surgical infection

47 **Abstract**

48  
49 *Staphylococcus aureus* is the major organism responsible for surgical implant infections.  
50 Antimicrobial treatment of these infections often fails leading to expensive surgical intervention  
51 and increased risk of mortality to the patient. The challenge in treating these infections is  
52 associated with the high tolerance of *S. aureus* biofilm to antibiotics. MazEF, a toxin-antitoxin  
53 system, is thought to be an important regulator of this phenotype, but its physiological function  
54 in *S. aureus* is controversial. Here, we examined the role of MazEF in developing chronic  
55 infections by comparing growth and antibiotic tolerance phenotypes in three *S. aureus* strains  
56 to their corresponding strains with disruption of *mazF* expression. Strains lacking *mazF*  
57 production showed increased biofilm growth, and decreased biofilm antibiotic tolerance.  
58 Deletion of *icaADBC* in the *mazF::tn* background suppressed the growth phenotype observed  
59 with *mazF*-disrupted strains, suggesting the phenotype was *ica*-dependent. We confirmed  
60 these phenotypes in our murine animal model. Loss of *mazF* resulted in increased bacterial  
61 burden and decreased survival rate compared to its wild-type strain demonstrating that loss of  
62 the *mazF* gene caused an increase in *S. aureus* virulence. Although lack of *mazF* gene  
63 expression increased *S. aureus* virulence, it was more susceptible to antibiotics *in vivo*.  
64 Combined, the ability of *mazF* to inhibit biofilm formation and promote biofilm antibiotic  
65 tolerance plays a critical role in transitioning from an acute to chronic infection that is difficult to  
66 eradicate with antibiotics alone.

67  
68 **Importance**

69 Surgical infections are one of the most common types of infections obtained in a hospital.  
70 *Staphylococcus aureus* is the most common pathogen associated with this infection. These  
71 infections are resilient and difficult to eradicate as the bacteria form a biofilm, a community of  
72 bacteria held together by an extracellular matrix. Compared to bacteria floating in liquid,  
73 bacteria in a biofilm are more resistant to antibiotics. The mechanism behind how bacteria  
74 develop this resistance and establish a chronic infection is unknown. We demonstrate that  
75 *mazEF*, a toxin-antitoxin gene, inhibits biofilm formation and promotes biofilm antibiotic  
76 tolerance which allows *S. aureus* to transition from an acute to chronic infection that cannot be  
77 eradicated with antibiotics but is less virulent. This gene not only makes the bacteria more  
78 tolerant to antibiotics but makes the bacteria more tolerant to the host.

79

80

## 81 Introduction

82

83 *Staphylococcus aureus* is a gram-positive pathogen associated with a variety of disease  
84 processes from self-limited abscesses to life-threatening sepsis. These episodes are typically  
85 acute, and resolve over a limited time-period with either minimal or high morbidity and mortality  
86 (1). An exception includes *S. aureus* related surgical infection, especially those associated with  
87 medical devices. Surgical site infection is one of the most common health-care associated  
88 infections (2). Unlike the majority of *S. aureus* infections, these infections can be chronic,  
89 indolent, and challenging to treat.

90

91 Periprosthetic joint infection illustrates this challenge. Total knee arthroplasty is a common  
92 surgical procedure, and the most common reason for failure is infection, termed periprosthetic  
93 joint infection (3, 4). *S. aureus* periprosthetic joint infection can be culture negative for  
94 prolonged periods (5, 6), has high failure rates above 50% once treatment is initiated (5), and a  
95 5-year mortality of 20% (7-9), higher than many common cancers (10). Similar to other surgical  
96 implant associated infections, the challenge in treating this disease involves the ability of *S.*  
97 *aureus* to develop a chronic biofilm associated infection tolerant to antibiotics (11, 12).

98

99 In gram-positive bacteria, the mechanisms behind biofilm antibiotic tolerance and the ability to  
100 form chronic infections are poorly understood. It is suspected that toxin-antitoxin systems play  
101 an important role in these processes. Toxin-antitoxin (TA) systems encode a stable toxin  
102 protein capable of interfering with vital cellular processes and a labile antitoxin that counteracts  
103 the toxin (13-15). In *S. aureus*, the most well studied of these is the *mazEF* module where  
104 *mazF* is a stable toxin that cleaves specific mRNA, and *mazE* is an unstable antitoxin that  
105 inhibits *mazF* (16). In gram negative and acid-fast species, this system has been associated  
106 with antibiotic tolerance (17) and virulence (18). In *S. aureus*, the *mazEF* phenotype is  
107 controversial and its physiologic function in the disease process is unknown

108

109 The objective of this study was to identify a phenotype associated with *mazEF* in the *S. aureus*  
110 disease process. We hypothesized that toxin-antitoxin systems like *mazEF* contribute to the  
111 ability to establish chronic infections and antibiotic tolerant biofilms. Disruption of *mazF*  
112 expression in three different *S. aureus* strains, resulted in increased biofilm formation and a  
113 loss of antibiotic tolerance as compared to their wild-type strains on surgical implant material.  
114 In planktonic culture, when *mazF* disruption did alter growth, this was associated with antibiotic  
115 tolerance. In our animal model, the absence of *mazF* resulted in a more acute, pathogenic  
116 infection that was more difficult to treat with antibiotics. These phenotypes demonstrated that  
117 *mazF* expression resulted in lower growth and metabolic activity from decreased biofilm  
118 formation that allowed a transition from an acute to chronic biofilm infection and increased  
119 antibiotic tolerance.

120

## 121 Results

122

### 123 Disruption of *mazF* is associated with increased biofilm formation on surgical implant 124 material

125 Toxin antitoxin systems are associated with bacteria growth arrest (19-21). We hypothesized  
126 that the lack of *mazF* would result in increased biofilm formation from preventing growth

127 inhibition. Mature *S. aureus* (USA300 JE2) biofilm was cultured on titanium rods and  
128 quantitative culture was performed to assess biofilm mass. Disruption of *mazF* had increased  
129 biofilm mass as compared to parental strains (Fig. 1). We observed similar results on two  
130 additional methicillin sensitive *S. aureus* (MSSA) strains deleted for *mazF*, Newman (22) and  
131 SH1000 (23) (Fig. S1). These experiments were repeated, and biofilm was cultured on  
132 polystyrene, and quantified with crystal violet assay. A loss of *mazF* expression again resulted  
133 in increased biofilm mass on fibrinogen-coated wells in all three strains as compared to wild  
134 type (Fig. S2). To confirm the observed phenotype of *mazF* in *S. aureus*, we restored *mazF*  
135 expression *in trans* and observed a decrease in biofilm formation (Fig. S3).

### 136 137 **Loss of *mazF* expression decreases biofilm antibiotic tolerance**

138 In gram negative bacteria, *mazEF* contributes to antibiotic tolerance and bacterial persisters  
139 (24-26). The role of *mazEF* and other toxin-antitoxin systems in *S. aureus* antibiotic tolerance  
140 is conflicting and unclear (27, 28). We hypothesized that *mazEF* would contribute to biofilm  
141 antibiotic tolerance in *S. aureus*. Biofilm antibiotic tolerance was compared between the  
142 methicillin resistant *S. aureus* (MRSA) strain JE2 and its corresponding strain disrupted for the  
143 *mazF* gene. Mature biofilm cultured on surgical implant material was exposed to 10x minimum  
144 inhibitory concentration (MIC) of vancomycin, and quantitative culture was used to assess  
145 remaining biofilm mass over three days. Loss of *mazF* expression had a statistically significant  
146 increased loss of biofilm mass as compared to the wild type control demonstrating that loss of  
147 *mazF* expression decreased biofilm antibiotic tolerance (Fig. 2). These results were confirmed  
148 in two additional strains, Newman and SH1000, using both cefazolin and vancomycin (Fig.  
149 S4). For all three strains, there was no statistical difference in MICs between the wild type and  
150 loss of function strains for cefazolin or vancomycin (Supplemental Table 1).

### 151 152 **Lack of *mazF* expression only altered planktonic antibiotic tolerance when doubling rate 153 was altered**

154 After observing these strong *mazF* biofilm phenotypes of increased biofilm formation and  
155 decreased antibiotic tolerance, we questioned if a similar pattern would be observed in  
156 planktonic culture. The growth rate of these three *S. aureus* strains were compared after  
157 exiting stationary phase. Loss of *mazF* expression resulted in a statistically significant  
158 increased early logarithmic planktonic growth rate in JE2 and SH1000 *S. aureus* strains, but  
159 this was not observed at each time point. When the early logarithmic doubling time was  
160 compared, only SH1000 and JE2 had a statistically increased doubling rate (Fig. 3A) and  
161 Newman did not. A similar pattern was observed with planktonic antibiotic tolerance; deletion  
162 or disruption of *mazF* only decreased antibiotic tolerance in the same strains that had an  
163 increase in doubling rate, JE2 and SH1000 (Figs. 3B, 3C).

### 164 165 **Loss of *mazF* expression did not alter *sigB* transcription**

166 The *sigB* operon is a master regulator in *S. aureus* that allows it to rapidly redirect  
167 transcriptional activities in response to stress (22). It has the potential to be a major regulator  
168 of *S. aureus* biofilm formation and virulence (29). The *sigB* operon is directly downstream from  
169 *mazEF*, and disruption of *mazF* expression could possibly alter *sigB* expression. We looked at  
170 *sigB* expression and genes upstream and downstream of *mazF* to verify that neighboring gene  
171 expression was not altered. Quantitative RT-PCR analysis demonstrated no change in  
172 expression of *sigB* and the *sigB* dependent gene, *asp23* (alkaline shock protein 23), between  
173 the three strains with loss of *mazF* expression and their respective wild type control (Fig. 4A

174 and B). We also examined the expression of the genes *rpoF*, *rsbW*, and *alr* which are directly  
175 upstream and downstream of *mazF*, based on genomic location and transcriptional order,  
176 using qRT-PCR. There was no statistically significant difference in *rpoF*, *rsbW* and *alr*  
177 expression between these strains and their wild type control (Fig. S5). These results  
178 demonstrate that loss of *mazF* did not alter expression of neighboring genes. The observed  
179 phenotype was related to the loss of *mazF* and not changes in *sigB* operon or other  
180 neighboring gene expression.

### 181 182 **Disruption of *mazF* increased pathogenicity, limited the ability of *S. aureus* to transition 183 from an acute to chronic infection, and inhibited antibiotic tolerance**

184 If lack of *mazF* expression increased biofilm formation, we hypothesized that this increased  
185 proliferation would result in increased disease severity. To test this hypothesis, we used a  
186 murine abscess model. After inoculation in the hind limb, quantitative culture was used to  
187 determine abscess bacterial burden at increasing time points in wild type and the *mazF::tn*  
188 strain. We selected the strain JE2 for these experiments as it was the most clinically relevant  
189 strain. In immune competent mice, loss of *mazF* had a similar phenotype to *in vitro*  
190 observations with increased proliferation and biofilm mass as compared to the wild type strain.  
191 After one week, the infection was on a downward trajectory after day 3 (Fig. 5A). To increase  
192 disease severity, we repeated experiments in neutropenic mice. Loss of *mazF* expression had  
193 increased proliferation and burden as compared to wild-type bacteria. Further, we observed a  
194 more virulent and aggressive infection. Wild type mice had almost 100% survival whereas  
195 mice inoculated with the *mazF* disrupted strain developed sepsis and death with survival at  
196 25% by day 7 (Fig. 5B). Surprisingly, although a more aggressive infection was observed, the  
197 *mazF* disrupted strain was more sensitive to antibiotics than the wild type control. After  
198 inoculation, there was a larger decrease in bacterial burden after treatment with vancomycin in  
199 the *mazF::tn strain* as compared to the wild type (Fig. 5C). Together these results supported  
200 the two *in vitro* phenotypes we observed, and suggest that *mazF* contributes to a phenotype of  
201 decreased virulence and pathogenesis.

### 202 203 **Increased biofilm formation in a *mazF*-disrupted strain is *ica*-dependent**

204 After a phenotype for *mazF* and a possible role in pathogenesis was identified, we attempted  
205 to identify a mechanism behind its regulatory control. The intercellular adhesion gene cluster  
206 (*ica*) is composed of *icaA*, *icaD*, *icaB* and *icaC*, and encodes proteins that promotes  
207 intercellular adhesion in many strains and species of *Staphylococcus* (30). Deletion of *mazF* in  
208 *S. aureus* results in increased biofilm formation that is *ica*-dependent (31). To test the  
209 hypotheses that the phenotype of increased growth and pathogenesis from loss of *mazF*  
210 expression was *ica*-dependent, we deleted the *icaADBC* genes from the *mazF::tn* strain to  
211 generate a *mazF::tn/ΔicaADBC* strain. *S. aureus mazF::tn/ΔicaADBC* strains had lower biofilm  
212 formation than the wild type and *mazF::tn* strains (Fig. 6A). The neutropenic murine abscess  
213 model was repeated with the *mazF::tn/ΔicaADBC* strain. The phenotype associated with loss  
214 of *mazF* expression was again suppressed. Mice inoculated with the *mazF::tn/ΔicaADBC* had  
215 comparable survival to the wild type control whereas the *mazF::tn* strain had 50% survival (Fig.  
216 6C). The *mazF::tn/ΔicaADBC* strain overcorrected the *mazF::tn* growth phenotype confirming  
217 the roles of *icaA*, *icaB*, *icaC* and *icaD* in *mazEF* function and suggests that these 4 genes are  
218 likely involved in controlling other process outside the *mazEF* system. The ability of the  
219 *mazF::tn/ΔicaADBC* strain to restore survival in the murine abscess model confirmed a role of  
220 *ica* control of biofilm formation in pathogenesis.

221  
222  
223  
224  
225  
226  
227  
228  
229  
230  
231  
232  
233  
234  
235  
236  
237  
238  
239  
240  
241  
242  
243  
244  
245  
246  
247  
248  
249  
250  
251  
252  
253  
254  
255  
256  
257  
258  
259  
260  
261  
262  
263  
264  
265  
266

## Decreased biofilm antibiotic tolerance in a *mazF* disruption is not *ica*-dependent

We then tested the role of *icaADBC* in regulating *mazF* biofilm antibiotic tolerance. Mature biofilm was exposed to 10x MIC vancomycin. *mazF::tn* and *mazF::tn/ΔicaADBC* strains had decreased vancomycin tolerance compared with wild type strain. Unlike the biofilm formation phenotype where deletion of *icaADBC* reversed the *mazF* disruption phenotype, loss of both *mazF* and *icaADBC* expression resulted in even less biofilm antibiotic tolerance than loss of *mazF* alone. This demonstrated that *ica* genes were also involved in antibiotic tolerance as well (Fig. 6B).

## Discussion

The physiologic role of bacterial toxin-antitoxin systems remain unknown. In *S. aureus*, *mazEF* is a well-studied toxin-antitoxin system whose phenotype and physiologic role in *S. aureus* remains elusive. Loss of *mazF* expression resulted in a phenotype of increased biofilm formation on surgical implant material and decreased biofilm antibiotic tolerance in all three *S. aureus* strains, but little change in planktonic cells. In our murine abscess model, the phenotypes associated with *mazEF* contributed to a biofilm-dependent disease process that is consistent with most chronic bacterial infections and the clinical manifestation of surgical infections. Further mechanistic analysis supported a role for extracellular polysaccharide adhesins in the increased biofilm formation and pathogenesis when *mazF* expression is disrupted. Combined, these results suggest that *mazEF* helps regulate the transition between acute to chronic infection in *S. aureus*.

Regulation of growth and biofilm formation is a phenotype associated with TA systems. The mechanism of toxin-antitoxin systems includes an antitoxin that prevents the toxin from inducing growth arrest using a variety of tools (24, 32). After loss of *mazF* expression, we observed increased biofilm when compared to its isogenic wild-type strain on fibrinogen-coated plastic and titanium *in vitro* and *in vivo*. This supports the work of other groups where overexpression of *mazF* in *S. aureus* resulted in growth arrest (21) and *mazF* mutants had increased biofilm formation (31). This is the primary mechanism where bacteria are thought to become antibiotic tolerant from toxin-antitoxin systems; dormant bacteria are tolerant to an antibiotic whose main process is disrupting their metabolism.

There is evidence to suggest that TA systems play an important role in antibiotic tolerance based on multiple examples in gram negative species (26) as well as in acid-fast mycobacterium (17). Although there is less evidence for this phenotype in gram-positive organisms, it has been suspected a similar pattern exists in *S. aureus*. We observed a difference in biofilm antibiotic tolerance when *mazF* expression was disrupted as compared to its wild type strains (Fig. 2). We did not observe a difference in the MIC. This supports similar previous observations (31). Other groups have noted that in *S. aureus* *mazF* transcription is altered by sub-MIC concentrations of MICs of tetracycline, penicillin, and linezolid (22). Despite generating greater biofilm formation, the loss of *mazF* expression demonstrated increased antibiotic susceptibility to clinically relevant antibiotics cefazolin and vancomycin. Combined this provides strong evidence for a major role of *mazF* in *S. aureus* biofilm antibiotic tolerance.

267 Persisters are a subpopulation of bacteria that have a phenotypic tolerance to antibiotics (33,  
268 34). The mechanism behind this tolerance is thought to be regulated by the metabolic state of  
269 the cell (35). We observed that the role of *mazF* in antibiotic tolerance appears to be correlated  
270 with growth. The phenotype of antibiotic tolerance was more weakly observed in planktonic *S.*  
271 *aureus* strains (Fig. 3). In planktonic culture, only loss of function strains with decreased  
272 doubling times as compared to the wild type strains were observed to have decreased  
273 planktonic antibiotic tolerance. This supports other results suggesting that persister formation  
274 is based on ATP levels, and is an area of future work. Likely, multiple mechanisms exist to  
275 support persister cell formation and antibiotic tolerance, including the stringent response (28).

276  
277 Biofilm formation is an important step for *S. aureus* to establish an infection. This is regulated  
278 by polysaccharide intercellular adhesin (PIA/PNAG) encoded by the *ica* operon (36). Based on  
279 this and our observation that loss of *mazF* expression increased biofilm formation, we  
280 speculated that *mazF* inhibits biofilm formation by decreasing *ica* transcription. A  
281 *mazF::tn/ΔicaADBC* strain reversed the *in vitro* and *in vivo* phenotypes from loss of *mazF*  
282 expression (Fig. 6). This *mazF::tn ΔicaADBC* strain had similar pathogenicity as the wild type  
283 strain. This provides evidence that *ica*-mediated biofilm formation and pathogenicity are  
284 inhibited by *mazF*. This supports other groups observations that *S. aureus* biofilm formation is  
285 dependent on *mazF* mRNA interferase activity (31).

286  
287 *S. aureus* infections are typically acute. Although there is a range of pathogenesis from simple,  
288 superficial abscesses to life threatening systemic sepsis, the outcomes of these disease  
289 processes resolve over a limited time period. An exception is surgical infection where chronic  
290 infections can develop over an extended period of time and biofilm formation plays an  
291 important physiologic role (5, 11). Regulation of growth, biofilm formation, and antibiotic  
292 tolerance could have important roles of bacteria physiology in this disease state. *S. aureus*  
293 biofilm formation is an essential step in establishing infection and pathogenicity (37, 38).  
294 Surprisingly, although loss of *mazF* created a more virulent organism with higher lethality,  
295 these infections were also more susceptible to antibiotics. Combined, these results suggest  
296 that *mazF* expression inhibits biofilm formation and increases antibiotic tolerance allowing the  
297 bacteria to transition to a chronic infection that is more challenging to treat. This demonstrates  
298 a physiologic role for toxin antitoxin systems during infections. *MazEF* toxin antitoxin systems  
299 not only make the bacteria more tolerant to antibiotics but makes the bacteria more tolerant to  
300 the host.

301

## 302 **Materials and Methods**

303

### 304 **Bacterial strains, plasmids and growth conditions**

305 USA 300 JE2 was selected as the primary strain as it was the most clinically relevant, and  
306 USA300 clones have the highest growth rate as compared to other common *S. aureus* strains  
307 (39). All bacterial strains and plasmids used in this study are listed in Table 1. *Staphylococcus*  
308 *aureus* strains were cultured in Trypticase soy broth (TSB) medium with or without antibiotics.

309

### 310 **Genomic bacterial DNA isolation**

311 Genomic DNA was isolated from *S. aureus* samples by following manufacturer's instructions  
312 (MasterPure gram positive DNA Purification Kit; Lucigen, USA). Briefly, a single colony from a  
313 TSB plate was inoculated in TSB medium and grown overnight at 37°C in an orbital shaker.

314 Pellet 1.5 ml culture and resuspend in 150  $\mu$ l TE buffer. Lysis the bacteria in lysis buffer at  
 315 37°C until bacterial cell wall is destroyed. Treated with Proteinase K. After added protein  
 316 precipitation reagent. Pellet the debris by centrifugation at 4°C for 10 minutes at 12,000 x g.  
 317 Keep the supernatant and pellet the genome DNA with isopropanol. Rinse the pellet with 70%  
 318 ethanol. Resuspend the DNA in TE Buffer. The genomic DNA can be used as template in  
 319 following PCR reactions.

320  
 321 Table 1 Bacterial stains and plasmids used in this study

Strain or plasmid	Genotype characteristics	and/or	Source reference	or
Strains				
RN4220	Heavily mutagenized NCTC 8325-4		Cheung (40)	
Newman-WT	Overexpresses <i>clfA</i> and <i>sae</i>		Cheung (22)	
Newman- $\Delta mazEF$	Newman $\Delta mazEF$		Cheung (22)	
SH1000-WT	Derived from NCTC 8325		Löffler (23)	
SH1000- $\Delta mazF$	SH1000 $\Delta mazF$		Cheung (22)	
JE2-WT	FPR3757 <i>pvl</i> positive		ATCC	
JE2- <i>mazF::tn</i>	NE1833, JE2 <i>mazF::tn</i>		Nebraska Tn Mutant Library	
JE2-WT-Spec	JE2 WT with empty spec vector		This study	
JE2-comp	JE2 <i>mazF</i> complement		This study	
JE2- <i>mazF::tn</i> / $\Delta ica$	JE2 <i>mazF::tn</i> / $\Delta icaADBC$		This study	
<i>E. coli</i> DH10B	General purpose competent cells for cloning		ThermoFisher Scientific	
Plasmids				
pKFT	5.7 kb temperature-sensitive shuttle vector; <i>Amp<sup>r</sup></i> , <i>Tet<sup>r</sup></i> in <i>E. coli</i> , <i>Tet<sup>r</sup></i> in <i>S. aureus</i>		Inouye (31)	
pLZ12-Spec	Shuttle vector with pWV01 origin; <i>Spec<sup>r</sup></i> in <i>E. coli</i> and <i>S. aureus</i>		(41)	
pFK74	pKFT containing regions upstream and downstream of the <i>icaADBC</i> genes		(31)	

322

### 323 Creation the *mazF* complementary strain

324 The complete *mazF* gene was amplified from 860 bp upstream of the *mazF* open reading  
 325 frame, including promoter region, in JE2 by PCR and cloned into a pLZ12-spec shuttle vector.  
 326 The transformed *mazF* expression vector was transformed into the *mazF::tn* strain and  
 327 selected with 200  $\mu$ g/ml spectinomycin.

328

### 329 Isolation of RNA and quantitative RT-PCR analysis

330 RNA isolation and quantitative reverse transcription polymerase chain reaction (RT-PCR) were  
 331 performed by following the manufacturer's instruction of the product. In brief, *S. aureus* was  
 332 grown in 4 mL of TSB medium supplemented with appropriate antibiotics at 37°C for 16 hours.  
 333 Overnight culture was centrifuged, and pellet resuspended in TE Buffer by vortexing. 500  
 334  $\mu$ g/ml lysostaphin (Sigma-Aldrich) was added to the resuspended bacteria and incubate at



335 37°C for 15 minutes. Total RNA was extracted using TRIzol® Max™ Bacterial RNA Isolation  
336 Kit (Thermo Fisher Scientific). Single-stranded cDNA was created from reverse transcription of  
337 the RNA using SuperScript IV Reverse Transcriptase (Thermo Fisher Scientific). The newly  
338 synthesized cDNA was used immediately or frozen at -80 °C.

339 Quantitative RT-PCR analysis was performed using the CFX96 Real-Time System (BioRad,  
340 Richmond, CA) and PowerUp™ SYBR Green Master Mix (Thermo Fisher Scientific). The  
341 cycling conditions were 50 °C for 10 min and 95 °C for 5 min, followed by 45 cycles of 95 °C for  
342 10 sec and 62 °C for 30 sec. For all samples, the threshold cycle number ( $C_t$ ) at which the  
343 fluorescence values became logarithmic was determined. The  $\Delta C_t$  value was calculated for  
344 each sample as the difference between the sample  $C_t$  and the control  $C_t$ .

### 345 346 **Creation of *icaADBC* gene deletion using pKFT Vector**

347 A JE2 double *mazF::tn/ΔicaADBC* strain was created from the base JE2 *mazF::tn* strain using  
348 a previously described protocol (42). Briefly, the allelic replacement vector pFK74 containing  
349 regions upstream 1.1kb and downstream 0.9 kb of the *icaADBC* gene was first transformed  
350 into DNA restriction system-deficient *S. aureus* RN4220, then a modified plasmid was isolated  
351 and electroporated into *mazF::tn* strain (NE1833) from NARSA NR-48501 library.  
352 Transformants were selected at 30 °C on TSB plates containing tetracycline. A single colony  
353 transformant was cultured at 30 °C in TSB media containing tetracycline in an orbital shaker.  
354 Integration of the plasmid into the chromosome by a single crossover event was achieved by  
355 incubation at 42 °C on TSB plates containing tetracycline. Correct homologous recombination  
356 of the target region was verified by PCR using primer set of pUC-UV (5'-  
357 CGACGTTGTAACGACGGCCAGT-3', plasmid) and *icaADBC* 5'-up (5'-  
358 CCATCACATAGGCGCTTATCAA-3', chromosome) or pUC-RV (5'-  
359 CATGGTCATAGCTGTTTCCTGTG-3', plasmid) and *icaADBC* 3'-dn (5'-  
360 GAAGCAACGCACAAAGCATTA-3', chromosome). Integrants were grown at 25 °C overnight  
361 with shaking in 10 ml TSB without any antibiotics. Bacteria was serially diluted and plated on  
362 TSB plates at 42 °C. The excision of the plasmid region in the chromosome by a second  
363 crossover event was screened for by isolation of tetracycline-sensitive colonies by replica-  
364 plating candidates on TSB plates versus TSB plates containing tetracycline (3 µg/ml).  
365 Integrants were cultured overnight at 37 °C. Then, the markerless deletion mutants were  
366 screened by PCR using primers *icaADBC*-1 (5'-AAAAGATCTTTAGTAGCGAATACTTC-  
367 3') and *icaADBC*-4 (5'-  
368 TACAAGATCTTTGGCATCATTTAGCAGAC-3') from tetracycline-sensitive colonies. The strain  
369 with *icaADBC* deletion was screened by PCR and confirmed by DNA sequencing.

### 370 371 **Cell growth curve and doubling time**

372 Approximately  $1 \times 10^6$  cells were added from overnight culture to fresh TSB medium and  
373 incubated at 37°C. The OD<sub>600</sub> absorbance (TECAN, infinite M200) was measured every hour  
374 during a 24 hour period. Calculation of the doubling time was based off of these  
375 measurements.

### 376 377 **Biofilm formation assay**

378 Four titanium rods (12 mm) per well were incubated in TSB growth medium inoculated with  
379  $1 \times 10^4$  CFU *S. aureus* for 24 to 96 hours. Titanium rods were then washed three times with 1ml  
380 PBS and then sonicated for 30 minutes in 1 ml fresh TSB medium. After serial 1:10 dilution,  
381 the bacterial concentration (CFU/mL) was determined via colony-forming unit (CFU) assay on

382 TSA II blood agar plates (Thermo Fisher Scientific, USA). A semi-quantitative adherence  
383 assay was performed on 96-well tissue culture polystyrene plates (Sigma-Aldrich, USA). Plates  
384 were coated with 200  $\mu$ l of phosphate-buffered saline (PBS) containing 5  $\mu$ g/ml fibrinogen  
385 (Sigma-Aldrich, USA) overnight at 4°C. Washed three times with PBS and then blocked with  
386 100  $\mu$ l of a 2% bovine serum albumin (BSA) solution for 1 h at 37°C. The wells were carefully  
387 washed three times with 100  $\mu$ l of PBS; 100  $\mu$ l of bacteria (approximately  $1 \times 10^7$  cells) was  
388 added to the appropriate wells and incubated for 24 hours at 37 °C. The wells were washed  
389 four times with 100  $\mu$ l of PBS. Bacteria were fixed with 100  $\mu$ l of 10 % formaldehyde (Sigma-  
390 Aldrich, USA) for 10 min. Then 100  $\mu$ l of 0.2% crystal violet (Sigma-Aldrich, USA) was added  
391 to each well for 10 min, cells were washed four times with distilled water. Air dried wells for 2  
392 hours and then add 100  $\mu$ l of 30% acetic acid (Fisher Scientific, USA) to dissolve crystal violet  
393 and the absorbance was measured at 590 nm.

394

#### 395 **Minimum inhibitory concentration (MIC) assay**

396 A single colony from an overnight agar plate was inoculated in 5 ml TSB medium to achieve  
397 the specified inoculum turbidity by comparing to a 0.5x McFarland turbidity standard ( $\sim 1 \times 10^8$   
398 CFU/ml). A sterile swab was placed in the inoculum suspension and streaked across the entire  
399 agar surface six times, rotating the plate to evenly distribute the inoculum. An Etest MIC test  
400 strips (Liofilchem, Italy) was applied with sterile forceps. Agar plates were then incubated in an  
401 inverted position at 37 °C overnight.

402

#### 403 **Biofilm and planktonic antibiotics tolerance assay**

404 For biofilm assay, grow *S. aureus* strains on surgical implant material (12mm titanium rods) for  
405 4 days to form mature biofilm (change medium every day). Then, exposed the mature biofilm  
406 to 10x MIC of cefazolin or vancomycin for 3 days (change medium every day). Implants were  
407 then washed, removed, sonicated, and plated to enumerate survivors (CFU assay) at each  
408 day. For planktonic assay, grow *S. aureus* strains in fresh TSB media overnight. Next day,  
409 1:100 diluted the overnight culture media with fresh TSB medium and grow to around 0.5X  
410 McFarland turbidity under 37°C. Do CFU assay to determine the viable cells before the  
411 treatment. Then, exposed the bacteria to 10X MIC cefazolin or vancomycin to 4-hour and 24-  
412 hour time point. And plated to enumerate survivors (CFU assay) at each time point. Calculate  
413 the percentage of survival (%) at each time point. All experiments were completed in triplicate.  
414 \*  $p < 0.05$ , \*\*  $p < 0.01$ . Error bars represent 95% CI (95% confidence interval).

415

#### 416 **Mice, Neutropenic Thigh model and *Staphylococcus aureus* strains administration**

417 Eight-week-old B57BL/6J mice were purchased from the Jackson laboratory (Bar Harbor, ME,  
418 USA). All animal protocols used for these experiments were approved by the University of  
419 Pittsburgh's Institutional Animal Care and Use Committee. Mice were rendered neutropenic by  
420 two 100  $\mu$ l intra peritoneal injections of cyclophosphamide (150 mg/kg three days pre-infection  
421 and 100 mg/kg one day pre-infection). Mice were anesthetized by 2% isoflurane, hair was  
422 removed from leg and treated with betadine. An inoculation volume of 100  $\mu$ l,  $1 \times 10^6$  CFU of  
423 JE2-WT or JE2- $\Delta mazF::tn$  strain was injected into the thigh. Mice were monitored for weight  
424 loss, leg swelling, ambulatory abilities, signs of sepsis, and death. Mice were sacrificed at 1, 3,  
425 and 7 days post infection. A  $\sim 5 \times 5$  mm piece of thigh muscle from infection site was obtained  
426 and placed into 1% Tween 20 in PBS on ice. Abscess samples were sonicated 10 minutes,  
427 and colony forming unit (CFU) assay was performed on blood agar plates to quantify bacterial  
428 burden.

429

## 430 **Statistical analysis**

431 Statistical analysis was based on the number of populations and comparisons. Student t-test  
432 was used for two populations. One-way anova and two-way anova was used for comparing  
433 multiple populations across either one condition or two conditions respectively. To determine  
434 antibiotic tolerance, multilevel mixed-effects linear regression models were constructed to  
435 compare the rate of change in CFU/mL over time between wild type and strains with loss of  
436 *mazF* expression. The outcome, CFU/mL, was natural-log transformed to produce  
437 approximately normally distributed values before fitting models via maximum likelihood  
438 estimation (MLE). Bacteria type (WT,  $\Delta mazF$ ), time, and a type-by-time interaction were  
439 included as fixed effects in the multilevel models, and the baseline concentration was  
440 accounted for. Random effects for Experiment, as well as Group (nested within Experiment),  
441 were included in all models to adjust for within-cluster correlation. Of primary interest were the  
442 type-by-time interaction coefficients, which reflect the degree to which the rate of decline in  
443 log-CFU differs between wildtype and  $\Delta mazF$  bacteria. After fitting the models, the estimated  
444 interaction coefficients were back-transformed to provide interpretable results on the original,  
445 non-logarithmic CFU/mL scale.

446

## 447 **Acknowledgements**

448 Dr. Kenneth Urish is supported in part by the National Institute of Arthritis and Musculoskeletal  
449 and Skin Diseases (NIAMS K08AR071494), the National Center for Advancing Translational  
450 Science (NCATS KL2TR0001856), and the Orthopaedic Research and Education Foundation.

451

## 452 **References**

453

- 454 1. **Lowy FD.** 1998. Staphylococcus aureus infections. N Engl J Med **339**:520-532.
- 455 2. **Magill SS, O'Leary E, Janelle SJ, Thompson DL, Dumyati G, Nadle J, Wilson LE,**  
456 **Kainer MA, Lynfield R, Greissman S, Ray SM, Beldavs Z, Gross C, Bamberg W,**  
457 **Sievers M, Concannon C, Buhr N, Warnke L, Maloney M, Ocampo V, Brooks J,**  
458 **Oyewumi T, Sharmin S, Richards K, Rainbow J, Samper M, Hancock EB, Leaprot**  
459 **D, Scalise E, Badrun F, Phelps R, Edwards JR, Emerging Infections Program**  
460 **Hospital Prevalence Survey T.** 2018. Changes in Prevalence of Health Care-  
461 Associated Infections in U.S. Hospitals. N Engl J Med **379**:1732-1744.
- 462 3. **Bozic KJ, Kurtz SM, Lau E, Ong K, Chiu V, Vail TP, Rubash HE, Berry DJ.** 2010.  
463 The epidemiology of revision total knee arthroplasty in the United States. Clin Orthop  
464 Relat Res **468**:45-51.
- 465 4. **Koh CK, Zeng I, Ravi S, Zhu M, Vince KG, Young SW.** 2017. Periprosthetic Joint  
466 Infection Is the Main Cause of Failure for Modern Knee Arthroplasty: An Analysis of  
467 11,134 Knees. Clin Orthop Relat Res **475**:2194-2201.
- 468 5. **Urish KL, Bullock AG, Kreger AM, Shah NB, Jeong K, Rothenberger SD, Infected**  
469 **Implant C.** 2018. A Multicenter Study of Irrigation and Debridement in Total Knee  
470 Arthroplasty Periprosthetic Joint Infection: Treatment Failure Is High. J Arthroplasty  
471 **33**:1154-1159.
- 472 6. **Yoon HK, Cho SH, Lee DY, Kang BH, Lee SH, Moon DG, Kim DH, Nam DC, Hwang**  
473 **SC.** 2017. A Review of the Literature on Culture-Negative Periprosthetic Joint Infection:  
474 Epidemiology, Diagnosis and Treatment. Knee Surg Relat Res **29**:155-164.

- 475 7. **Zmistowski B, Karam JA, Durinka JB, Casper DS, Parvizi J.** 2013. Periprosthetic  
476 joint infection increases the risk of one-year mortality. *J Bone Joint Surg Am* **95**:2177-  
477 2184.
- 478 8. **Choi HR, Bedair H.** 2014. Mortality following revision total knee arthroplasty: a matched  
479 cohort study of septic versus aseptic revisions. *J Arthroplasty* **29**:1216-1218.
- 480 9. **Lum ZC, Natsuhara KM, Shelton TJ, Giordani M, Pereira GC, Meehan JP.** 2018.  
481 Mortality During Total Knee Periprosthetic Joint Infection. *J Arthroplasty* **33**:3783-3788.
- 482 10. **Kurtz SM, Lau EC, Son MS, Chang ET, Zimmerli W, Parvizi J.** 2018. Are We Winning  
483 or Losing the Battle With Periprosthetic Joint Infection: Trends in Periprosthetic Joint  
484 Infection and Mortality Risk for the Medicare Population. *J Arthroplasty* **33**:3238-3245.
- 485 11. **Ma D, Shanks RMQ, Davis CM, 3rd, Craft DW, Wood TK, Hamlin BR, Urish KL.**  
486 2018. Viable bacteria persist on antibiotic spacers following two-stage revision for  
487 periprosthetic joint infection. *J Orthop Res* **36**:452-458.
- 488 12. **Urish KL, DeMuth PW, Kwan BW, Craft DW, Ma D, Haider H, Tuan RS, Wood TK,**  
489 **Davis CM, 3rd.** 2016. Antibiotic-tolerant *Staphylococcus aureus* Biofilm Persists on  
490 Arthroplasty Materials. *Clin Orthop Relat Res* **474**:1649-1656.
- 491 13. **Van Melder L, Saavedra De Bast M.** 2009. Bacterial toxin-antitoxin systems: more  
492 than selfish entities? *PLoS Genet* **5**:e1000437.
- 493 14. **Fozo EM, Makarova KS, Shabalina SA, Yutin N, Koonin EV, Storz G.** 2010.  
494 Abundance of type I toxin-antitoxin systems in bacteria: searches for new candidates  
495 and discovery of novel families. *Nucleic Acids Res* **38**:3743-3759.
- 496 15. **Gerdes K.** 2000. Toxin-antitoxin modules may regulate synthesis of macromolecules  
497 during nutritional stress. *J Bacteriol* **182**:561-572.
- 498 16. **Zhang Y, Zhang J, Hoeflich KP, Ikura M, Qing G, Inouye M.** 2003. MazF cleaves  
499 cellular mRNAs specifically at ACA to block protein synthesis in *Escherichia coli*. *Mol*  
500 *Cell* **12**:913-923.
- 501 17. **Tiwari P, Arora G, Singh M, Kidwai S, Narayan OP, Singh R.** 2015. MazF  
502 ribonucleases promote *Mycobacterium tuberculosis* drug tolerance and virulence in  
503 guinea pigs. *Nat Commun* **6**:6059.
- 504 18. **Tiwari P, Arora G, Singh M, Kidwai S, Narayan OP, Singh R.** 2015. Corrigendum:  
505 MazF ribonucleases promote *Mycobacterium tuberculosis* drug tolerance and virulence  
506 in guinea pigs. *Nat Commun* **6**:7273.
- 507 19. **Gerdes K, Christensen SK, Lobner-Olesen A.** 2005. Prokaryotic toxin-antitoxin stress  
508 response loci. *Nat Rev Microbiol* **3**:371-382.
- 509 20. **Korch SB, Malhotra V, Contreras H, Clark-Curtiss JE.** 2015. The *Mycobacterium*  
510 *tuberculosis* relBE toxin:antitoxin genes are stress-responsive modules that regulate  
511 growth through translation inhibition. *J Microbiol* **53**:783-795.
- 512 21. **Fu Z, Tamber S, Memmi G, Donegan NP, Cheung AL.** 2009. Overexpression of  
513 MazFsa in *Staphylococcus aureus* induces bacteriostasis by selectively targeting  
514 mRNAs for cleavage. *J Bacteriol* **191**:2051-2059.
- 515 22. **Donegan NP, Cheung AL.** 2009. Regulation of the mazEF toxin-antitoxin module in  
516 *Staphylococcus aureus* and its impact on sigB expression. *J Bacteriol* **191**:2795-2805.
- 517 23. **Tuchscher L, Medina E, Hussain M, Volker W, Heitmann V, Niemann S, Holzinger**  
518 **D, Roth J, Proctor RA, Becker K, Peters G, Loffler B.** 2011. *Staphylococcus aureus*  
519 phenotype switching: an effective bacterial strategy to escape host immune response  
520 and establish a chronic infection. *EMBO Mol Med* **3**:129-141.

- 521 24. **Wang X, Wood TK.** 2011. Toxin-antitoxin systems influence biofilm and persister cell  
522 formation and the general stress response. *Appl Environ Microbiol* **77**:5577-5583.
- 523 25. **Lewis K.** 2008. Multidrug tolerance of biofilms and persister cells. *Curr Top Microbiol*  
524 *Immunol* **322**:107-131.
- 525 26. **Tripathi A, Dewan PC, Siddique SA, Varadarajan R.** 2014. MazF-induced growth  
526 inhibition and persister generation in *Escherichia coli*. *J Biol Chem* **289**:4191-4205.
- 527 27. **Schuster CF, Mechler L, Nolle N, Krismer B, Zelder ME, Gotz F, Bertram R.** 2015.  
528 The MazEF Toxin-Antitoxin System Alters the beta-Lactam Susceptibility of  
529 *Staphylococcus aureus*. *PLoS One* **10**:e0126118.
- 530 28. **Conlon BP, Rowe SE, Gandt AB, Nuxoll AS, Donegan NP, Zalis EA, Clair G,  
531 Adkins JN, Cheung AL, Lewis K.** 2016. Persister formation in *Staphylococcus aureus*  
532 is associated with ATP depletion. *Nat Microbiol* **1**:16051.
- 533 29. **Mitchell G, Fugere A, Pepin Gaudreau K, Brouillette E, Frost EH, Cantin AM,  
534 Malouin F.** 2013. SigB is a dominant regulator of virulence in *Staphylococcus aureus*  
535 small-colony variants. *PLoS One* **8**:e65018.
- 536 30. **Cramton SE, Gerke C, Schnell NF, Nichols WW, Gotz F.** 1999. The intercellular  
537 adhesion (*ica*) locus is present in *Staphylococcus aureus* and is required for biofilm  
538 formation. *Infect Immun* **67**:5427-5433.
- 539 31. **Kato F, Yabuno Y, Yamaguchi Y, Sugai M, Inouye M.** 2017. Deletion of *mazF*  
540 increases *Staphylococcus aureus* biofilm formation in an *ica*-dependent manner. *Pathog*  
541 *Dis* **75**.
- 542 32. **Page R, Peti W.** 2016. Toxin-antitoxin systems in bacterial growth arrest and  
543 persistence. *Nat Chem Biol* **12**:208-214.
- 544 33. **Brauner A, Fridman O, Gefen O, Balaban NQ.** 2016. Distinguishing between  
545 resistance, tolerance and persistence to antibiotic treatment. *Nat Rev Microbiol* **14**:320-  
546 330.
- 547 34. **Balaban NQ, Merrin J, Chait R, Kowalik L, Leibler S.** 2004. Bacterial persistence as a  
548 phenotypic switch. *Science* **305**:1622-1625.
- 549 35. **Zampieri M, Enke T, Chubukov V, Ricci V, Piddock L, Sauer U.** 2017. Metabolic  
550 constraints on the evolution of antibiotic resistance. *Mol Syst Biol* **13**:917.
- 551 36. **Fluckiger U, Ulrich M, Steinhuber A, Doring G, Mack D, Landmann R, Goerke C,  
552 Wolz C.** 2005. Biofilm formation, *icaADBC* transcription, and polysaccharide  
553 intercellular adhesin synthesis by staphylococci in a device-related infection model.  
554 *Infect Immun* **73**:1811-1819.
- 555 37. **Costerton JW.** 1999. Introduction to biofilm. *Int J Antimicrob Agents* **11**:217-221;  
556 discussion 237-219.
- 557 38. **Donlan RM.** 2001. Biofilm formation: a clinically relevant microbiological process. *Clin*  
558 *Infect Dis* **33**:1387-1392.
- 559 39. **Thurlow LR, Joshi GS, Richardson AR.** 2012. Virulence strategies of the dominant  
560 USA300 lineage of community-associated methicillin-resistant *Staphylococcus aureus*  
561 (CA-MRSA). *FEMS Immunol Med Microbiol* **65**:5-22.
- 562 40. **Nair D, Memmi G, Hernandez D, Bard J, Beaume M, Gill S, Francois P, Cheung AL.**  
563 2011. Whole-genome sequencing of *Staphylococcus aureus* strain RN4220, a key  
564 laboratory strain used in virulence research, identifies mutations that affect not only  
565 virulence factors but also the fitness of the strain. *J Bacteriol* **193**:2332-2335.

- 566 41. **Husmann LK, Scott JR, Lindahl G, Stenberg L.** 1995. Expression of the Arp protein,  
567 a member of the M protein family, is not sufficient to inhibit phagocytosis of  
568 *Streptococcus pyogenes*. *Infect Immun* **63**:345-348.  
569 42. **Kato F, Sugai M.** 2011. A simple method of markerless gene deletion in  
570 *Staphylococcus aureus*. *J Microbiol Methods* **87**:76-81.  
571

## 572 **Supporting information**

### 573 **Figure legends**

#### 574 **Figure 1. Loss of *mazF* expression increases biofilm formation on surgical implant** 575 **material in *S. aureus*.**

576 Biofilm was cultured on surgical implant material (titanium rods, 12mm) for 4 days to form  
577 mature biofilm, and the biofilm growth was quantified by sonication, plating, and enumeration  
578 for USA 300 JE2. Experiments were completed in triplicate. \*\* p<0.01. Error bars represent  
579 95% CI (95% confidence interval).  
580

#### 581 **Figure 2. Loss of *mazF* expression decreases biofilm antibiotic tolerance in *S. aureus*.**

582 Mature JE2 biofilm was cultured on surgical implant material (4 days on 12mm titanium rods),  
583 and exposed to 10x MIC of vancomycin. Implants were then removed, sonicated, and plated to  
584 enumerate survivors on a daily basis over 3 days. Remaining biofilm on surgical implant  
585 material at each day was compared to the respective pretreated strain. All experiments were  
586 completed in triplicate. \*\* p<0.01. Error bars represent 95% confidence intervals.  
587

#### 588 **Figure 3. Loss of *mazF* expression increased planktonic growth and decreased** 589 **vancomycin and cefazolin planktonic antibiotics tolerance in *S. aureus*.**

590 (A) Based on the cell growth curve, the doubling time of each strain was determined.  
591 Disruption of *mazF* from *S. aureus* resulted in a shorter doubling time in JE2 and SH1000  
592 strains. (B) Disruption of *mazF* expression decreased the cefazolin planktonic antibiotics  
593 tolerance in SH1000. The strain JE2 was not included in these experiments as it is methicillin  
594 resistant. (C) Disruption of *mazF* expression decreased the planktonic vancomycin tolerance in  
595 JE2 and SH1000 strains. All experiments were completed in triplicate. \* p<0.05, \*\* p<0.01.  
596 Error bars represent 95% CI (95% confidence interval).  
597

#### 598 **Figure 4. Loss of *mazF* expression had no effect on *sigB* expression**

599 Quantitative real-time RT-PCR analysis of (A) *sigB* and (B) *asp23* expression in three *S.*  
600 *aureus* strains (JE2, Newman, and SH1000).  $\Delta C_t$  value were used to quantify gene expression  
601 levels. No significant differences in *sigB* or *asp23* expression were observed between the wild  
602 type and loss of *mazF* expression in all three *S. aureus* strains.  
603

#### 604 **Figure 5. Loss of *mazF* expression increases pathogenicity and limits *S. aureus* ability** 605 **to establish chronic infection**

606  
607  
608  
609  
610  
611  
612

613 Bacterial abscess burden and animal survival were used to test the pathogenicity of *S. aureus*  
614 wild type and its corresponded *mazF::tn* strains. (A) In both neutropenic and  
615 immunocompetent groups, loss of *mazF* increases bacterial burden compared to wild type  
616 strains which was most apparent at three days post infection (\*\*  $P < 0.01$ ). (B) Mortality in  
617 neutropenic mice inoculated with strains that had no *mazF* expression was 25% on day three  
618 and 75% on day seven post infection. Mice inoculated with wild type strain had 0% mortality at  
619 day 3 and 10% mortality at day 7. (C) The strain that lost *mazF* expression was more sensitive  
620 to antibiotics than the wild type control. After treatment with vancomycin, the loss of *mazF*  
621 expression had a 5 log reduction in biofilm as compared to the wild type strain (\*\*  $P < 0.01$ ).  
622

### 623 **Figure 6. Increased biofilm formation in the *mazF* disruption strain is *ica*-dependent**

624  
625 Biofilm formation in the *mazF::tn* and *mazF::tn/ΔicaADBC* strain were compared to the  
626 parental strain. (A) Biofilm formation of the *mazF::tn/ΔicaADBC* strain was lower than that of  
627 strains lacking *mazF* expression alone. (B) Biofilm antibiotic tolerance of the double loss of  
628 function was lower than that of strains lacking *mazF* expression alone. (C). *mazF/icaADBC*  
629 double loss of function strain reversed the animal mortality to wild type strain levels. All  
630 experiments were completed in triplicate. \*\*  $p < 0.01$ . Error bars represent 95% CI (95%  
631 confidence interval).  
632

### 633 **Supplemental Figure 1. Loss of *mazF* increases biofilm formation on surgical implant** 634 **material in *S. aureus*.**

635  
636 Biofilm was cultured on surgical implant material (titanium rods, 12 mm) for 4 days to form  
637 mature biofilm, and the biofilm growth was quantified by sonication, plating, and enumeration  
638 for JE2, Newman and SH1000 strains, respectively. All experiments were completed in  
639 triplicate. \*\*  $p < 0.01$ . Error bars represent 95% CI (95% confidence interval).  
640

### 641 **Supplemental Figure 2. Bacterial biofilm formation on 96-well culture plate**

642  
643 *S. aureus* strains were cultured on fibrinogen coated 96-well polystyrene plates for 24 to 48  
644 hours. Biofilm formation was quantified using the crystal violet method, the absorbance was  
645 measured at 590 nm. All experiments were completed in triplicate. \*\*  $p < 0.01$ . Error bars  
646 represent 95% CI (95% confidence interval).  
647

### 648 **Supplemental Figure 3. MazF complement reduces the planktonic cell growth and** 649 **biofilm formation**

650  
651 A genomic complement approach was used to restore *mazF* expression in JE2, and the  
652 growth phenotype was reversed. JE2 wild type strain with empty spec vector as a control.  
653 Biofilm formation measured by using the crystal violet assay (A) and titanium rods CFU assay  
654 (B) and planktonic growth measured using optical density (C) demonstrated that biofilm  
655 formation and planktonic growth was decreased in the *mazF* complement strain. All  
656 experiments were completed in triplicate. \*  $p < 0.05$ , \*\*  $p < 0.01$ . Error bars represent 95% CI  
657 (95% confidence interval).  
658

659 **Supplemental Figure 4. Loss of *mazF* decreases biofilm vancomycin and cefazolin**  
660 **tolerance in *S. aureus*.**

661  
662 Mature biofilm grown on surgical implant material (4 days on titanium rods) was exposed to  
663 10x MIC of cefazolin or vancomycin. Implants were then removed, sonicated, and plated to  
664 enumerate survivors on a daily basis over 3 days. A regression model was used to estimate  
665 the overall percent of biofilm remaining at day 3 relative to pretreated. (A) Biofilm of Newman  
666 and SH1000 strains were exposed to cefazolin. JE2 was not included as it is a MRSA. (B)  
667 Biofilm of JE2, Newman, and SH1000 strains were exposed to vancomycin. All experiments  
668 were completed in triplicate. \*  $p < 0.05$ , \*\*  $p < 0.01$ . Error bars represent 95% confidence  
669 intervals.

670  
671 **Supplemental Figure 5. Deletion of *mazF* had no effect on *sigB* operon expression**

672  
673 Quantitative real-time RT-PCR analysis of the *sigB* operon with *rpoF*, *rsbW*, and *alr* transcripts.  
674  $\Delta C_t$  value was used to indicate the expression levels of selected genes.

675  
676 Supplemental Table 1 Cefazolin and vancomycin MICs of non-biofilm *S. aureus*

Strains	MICs of Cefazolin (means $\pm$ SD) ( $\mu$ g/ml)	MICs of vancomycin (means $\pm$ SD) ( $\mu$ g/ml)
Newmen-WT	0.29 $\pm$ 0.08	2.33 $\pm$ 0.58
Newmen- $\Delta mazEF$	0.34 $\pm$ 0.08	2.67 $\pm$ 0.58
SH1000-WT	0.12 $\pm$ 0.02	1.67 $\pm$ 0.29
SH1000- $\Delta mazF$	0.12 $\pm$ 0.00	1.83 $\pm$ 0.29
JE2-WT	ND	1.08 $\pm$ 0.38
JE2- <i>mazF</i> :tn	ND	0.92 $\pm$ 0.14

677 The MIC difference between the *mazF* loss of function and wild type strains is not significant  
678 ( $p > 0.25$ ). ND indicates not determined as JE2 is a methicillin resistant strain of *S. aureus*.  
679



Figure 1. Deletion of *mazF* increases biofilm growth on surgical implant material

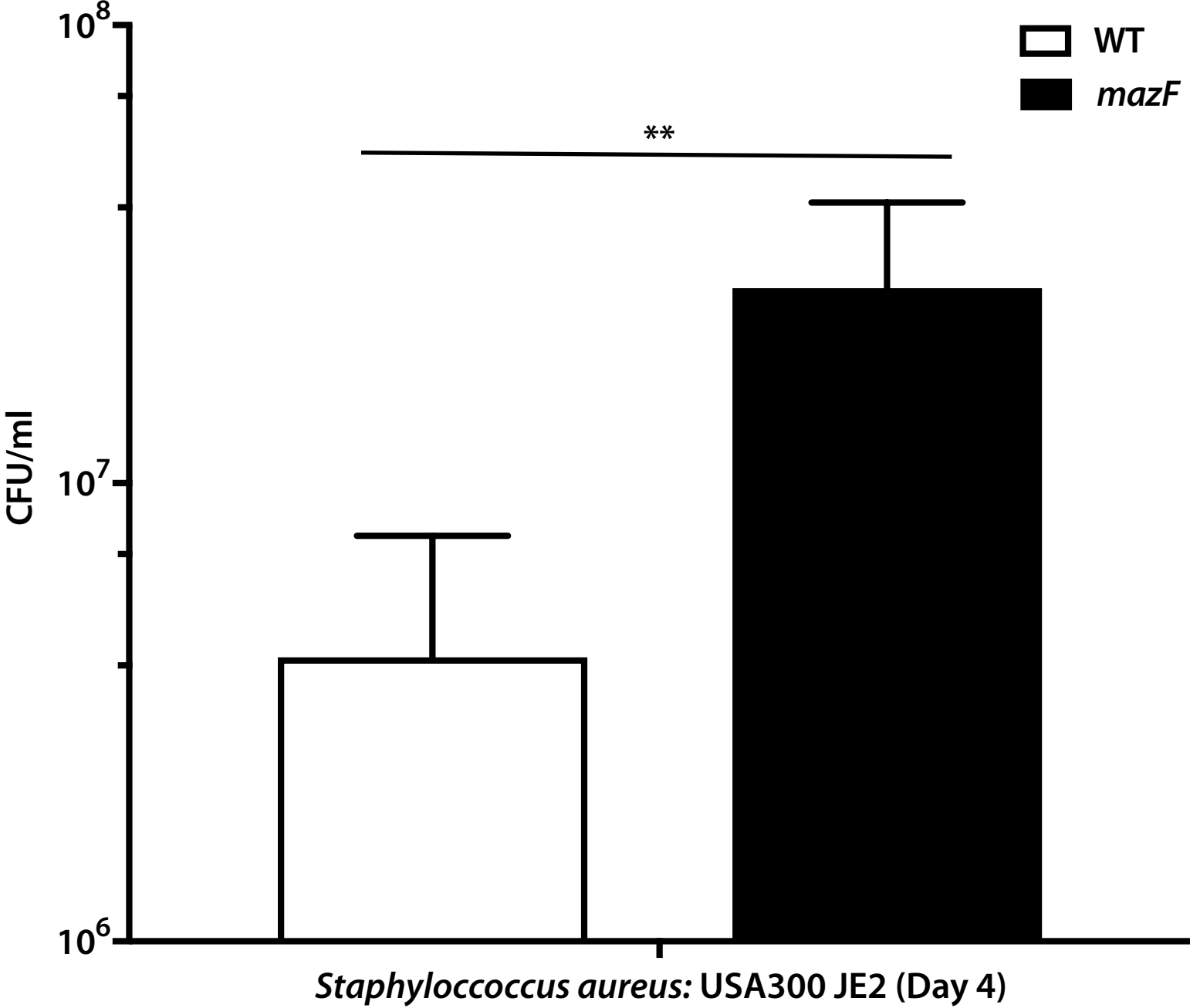
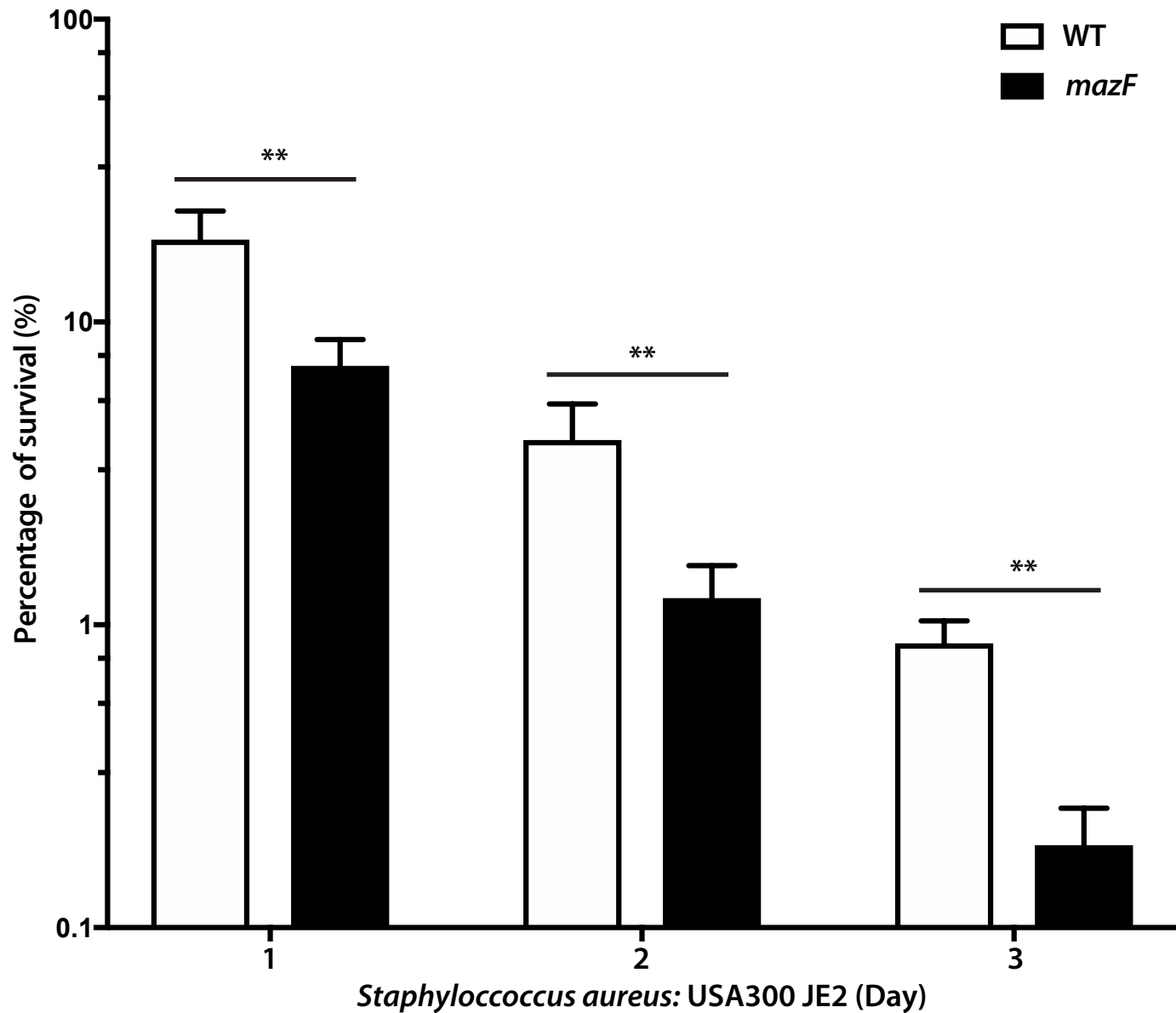


Figure 2. Deletion of *mazF* decreases the biofilm vancomycin tolerance



# Figure 3. Planktonic growth and antibiotic tolerance

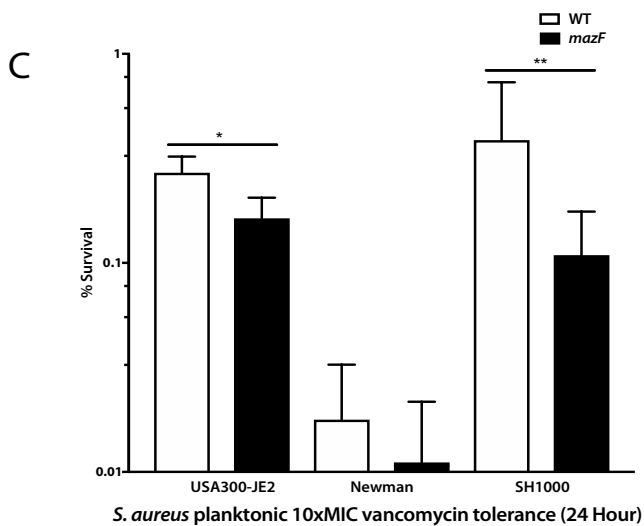
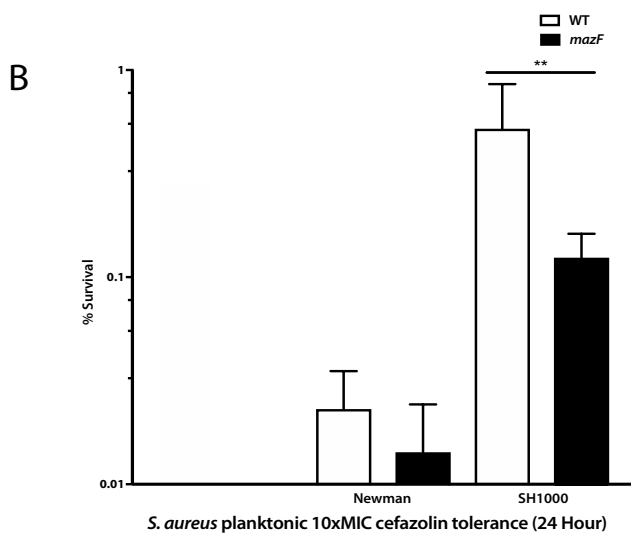
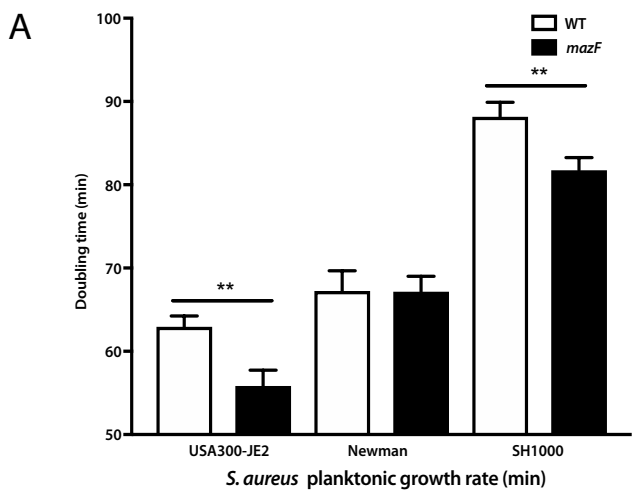
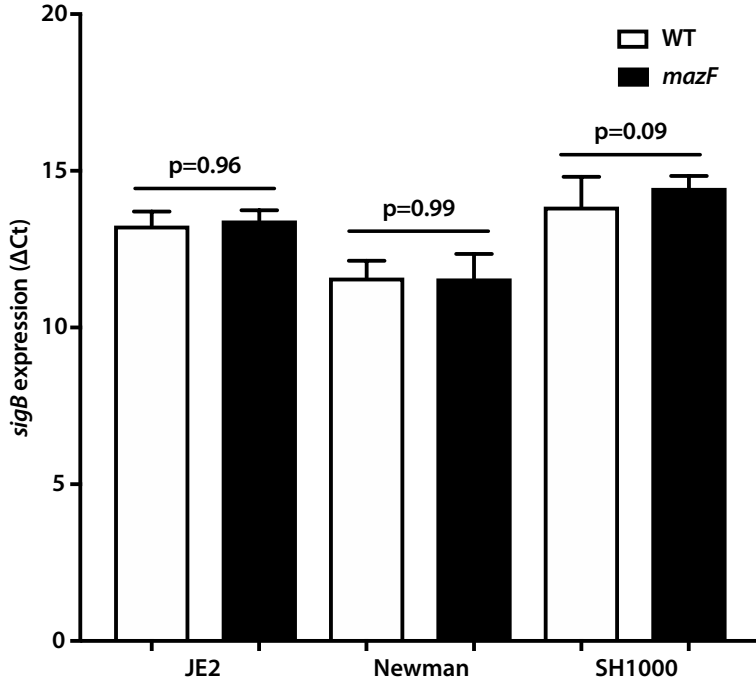
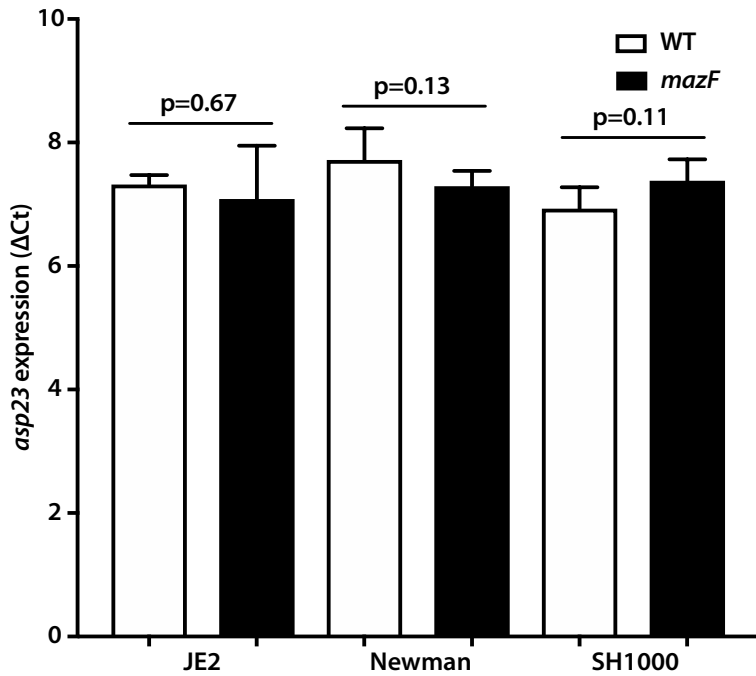


Figure 4. Deletion of *mazF* had no effect on the *sigB* expression ( $\Delta$ Ct)

A



B



**Figure 5. Deletion of *mazF* increases pathogenicity and limits the ability of *S. aureus* to establish a chronic infection**

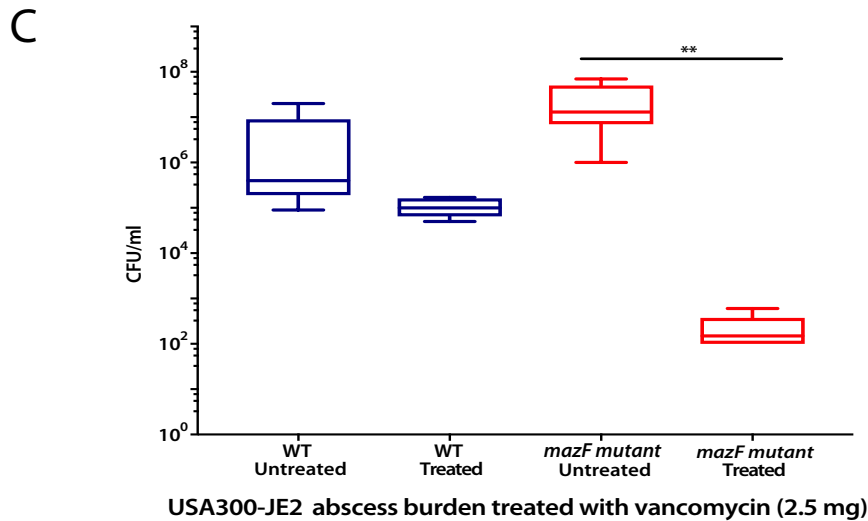
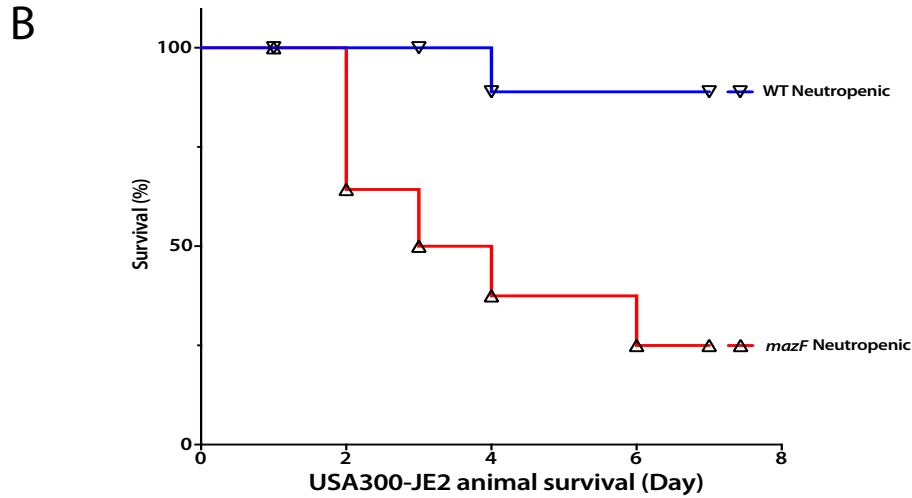
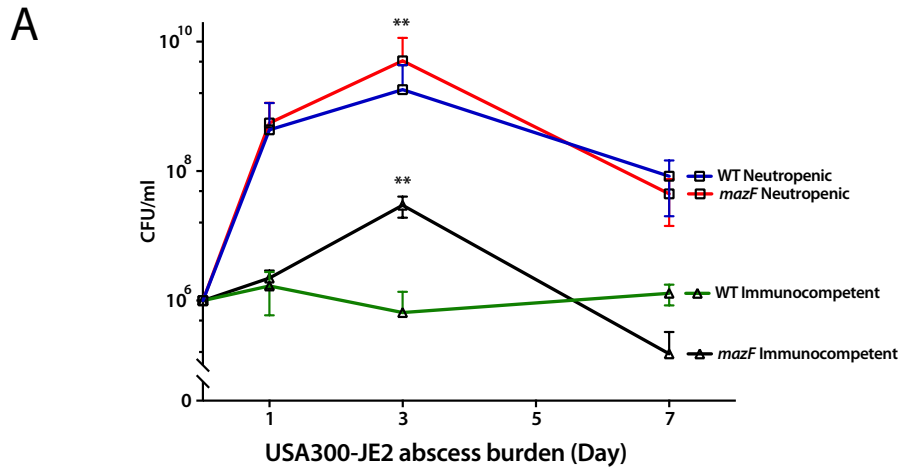
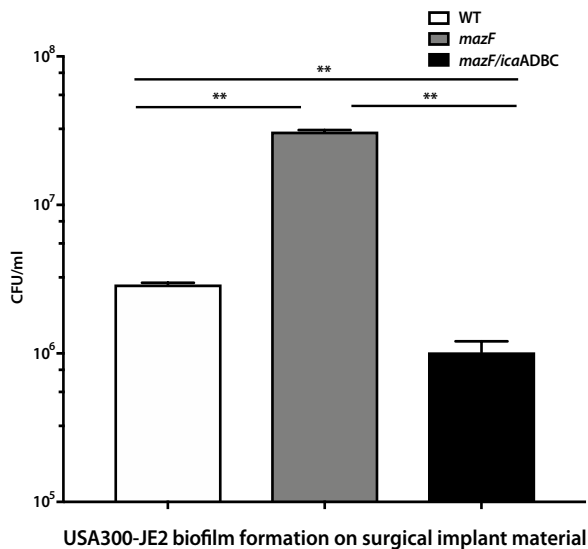
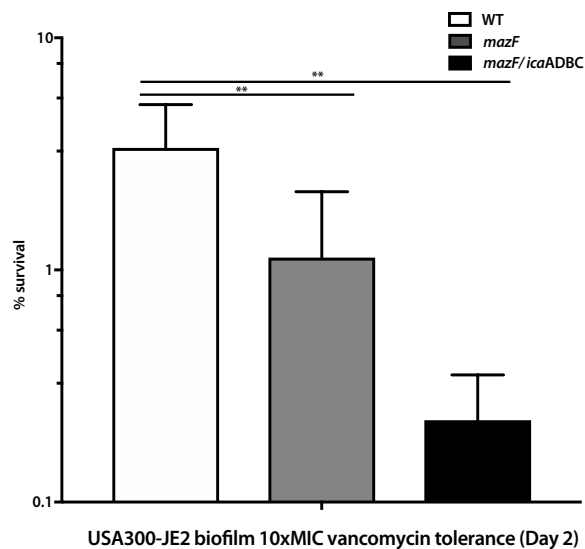


**Figure 6. Increased biofilm formation in the USA300-JE2 *mazF* deletion strain is *ica*-dependent**

**A**



**B**



**C**

